Smart Structures and Systems, *Vol. 25, No. 6* (*2020*) *693-705*
DOI: https://doi.org/10.12989/sss.2020.25.6.693

Large amplitude free vibrations of FGM shallow curved tubes in thermal environment

Hadi Babaei [1], Yaser Kiani*[2] and M. Reza Eslami [3]

[1] *Department of Mechanical Engineering*, *South Tehran Branch*, *Islamic Azad University*, *Tehran*, *Iran*
[2] *Faculty of Engineering*, *Shahrekord University*, *Shahrekord*, *Iran*
[3] *Mechanical Engineering Department*, *Amirkabir University of Technology*, *Tehran*, *Iran*

(*Received September 6, 2019, Revised December 20, 2019, Accepted January 23, 2020*)

Abstract. In the current investigation, large amplitude free vibration behavior of shallow curved pipes (tubes) made of functionally graded materials is investigated. Properties of the tube are distributed across the radius of the tube and are obtained by means of a power law function. It is also assumed that all thermo-mechanical properties are temperature dependent. The governing equations of the tube are obtained using a higher order shear deformation tube theory, where the traction free boundary conditions are satisfied on the top and bottom surfaces of the tube. The von Kármán type of geometrical non-linearity is included into the formulation to consider the large displacements and small strains. Uniform temperature elevation of the tube is also included into the formulation. For the case of tubes which are simply supported in flexure and axially immovable, the governing equations are solved using the two-step perturbation technique. Closed form expressions are provided to obtain the small and large amplitude fundamental natural frequencies of the FGM shallow curved tubes in thermal environment. Numerical results are given to explore the effects of thermal environment, radius ratio, and length to thickness ratio of the tube on the fundamental linear and non-linear frequencies.

Keywords: nonlinear free vibration; FGM; shallow curved tube; von Kármán nonlinearity; two-step perturbation method; thermal environment

1. Introduction

Functionally graded material (FGM) structures are commonly used in engineering applications (Wu and Li 2012, Wu and Liu 2013, Arefi 2015, Chen 2018). The FG material is a new advanced class of non-homogeneous composite materials which is usually made from a mixture of metal and ceramic.

Many investigations on the geometrically nonlinear analysis of buckling, post-buckling, and free vibrations of thin-walled FGM structures are available in the literature, see e.g., the book by Eslami (2018). In this book, nonlinear governing differential equations of various thin-walled structures made of different materials are solved using either analytical or numerical methods for several types of boundary conditions. Using the two-step perturbation technique, Shen (2011) obtained the analytical closed-form solutions as the sum of static solution and dynamic one of a homogeneous isotropic beam. In this study, nonlinear analysis of bending, post-buckling, and free vibrations of flat beams resting on elastic foundation are performed. Thai and Vo (2012) introduced the analytical closed-form solutions for bending and free vibration analysis of an FGM beam based on various higher order shear deformation theories. In this work, Navier solution procedure is used to solve the static and dynamic governing equations for simply supported boundary conditions. Zhang (2014) carefully examined the static and dynamic responses of the functionally graded material beams utilizing the Ritz method considering the thermal effects. In this study, thermal post-buckling and nonlinear free vibration problems of the FGM beams with immovable pinned and fixed ends are analyzed based on the physical neutral plane and higher order shear deformation theories.

Many studies on the static and dynamic behaviors of cylindrical flat beams/tubes made of functionally graded materials are also available in the following works.

Among them, Huang and Li (2010a) presented a study on the linear mechanical buckling of circular cylindrical5 beams made of functionally graded materials subjected to axial compressive load at the movable end of the beam. In this study, an analytical closed-form solution is obtained for critical buckling loads of cylindrical beams with movable simply supported boundary conditions. Nonlinear thermally induced responses of circular tubes made of FG materials subjected to uniform temperature rise loading are analyzed by Fu *et al*. (2015) based on a refined beam model. In this work, they used two analytical methods for linear thermal buckling and nonlinear thermal post-buckling problems of the FGM tubes with immovable simply supported end conditions. Also, thermal post-buckling and nonlinear bending problems are analysed using a two-step perturbation method for an FGM flat tube with clamped boundary conditions by She *et al*. (2017). Chen *et al*. (2017)

*Corresponding author, Assistant Professor,
E-mail: y.kiani@aut.ac.ir

ISSN: 1738-1584 (Print), 1738-1991 (Online)

performed the forced vibration analysis of an FGM flat tube resting on nonlinear elastic foundation in thermal environment. Nonlinear dynamic responses of the FGM flat tubes subjected to a moving load with constant velocity are analysed. In this study, the Galerkin and Newmark approximate methods are utilized to obtain the dynamic deflection responses of the FGM tube. Based on the nonlocal strain gradient and higher order shear deformation theories, She *et al*. (2018a) analyzed the functionally graded porous tubes. In this work, nonlinear bending and free vibration responses of the FG porous nanotubes are obtained using the two-step perturbation method for simply supported boundary conditions. Sharifi and She (2018) used a numerical method, i.e., the generalized differential quadrature method (GDQM), to obtain the free vibration response of the pre/post-buckled FGM nanotubes subjected to uniform temperature distribution. In this study, material properties are considered to be temperature-dependent. Babaei *et al*. (2019a, b) studied the thermal and mechanical post-buckling behaviors of geometrically imperfect FGM tubes surrounded by nonlinear elastic medium with clamped and pinned boundary conditions. Finally, She *et al*. (2019) presented a study on the hygro-thermal wave propagation of functionally graded double-layered nanotubes based on the strain gradient theory using an analytical method.

Also, many investigations on the static and dynamic responses of thin-walled curved beam structures and shallow arches made of functionally graded materials are available in the following studies.

For instance, Babaei *et al*. (2018a, b, c) analyzed the thermomechanical nonlinear static responses of the FGM shallow curved structures with rectangular and circular cross sections based on the higher order shear deformation theory. Snap-through type of instability and thermal bending of the structures with pinned/clamped boundary conditions are investigated. A two-step perturbation technique is utilized to solve the equilibrium equations of the FG shallow curved structures.

Based on the first-order shear deformation arch theory, Malekzadeh *et al*. (2009, 2010) investigated the in-plane and out-of-plane free vibration behaviors of functionally graded circular arches. In these studies, dynamic responses of FGM arches with temperature-dependent properties subjected to thermal environment are obtained using the generalized differential quadrature method (GDQM). Also, Piovan *et al*. (2012) presented a study on the in-plane and out-of-plane static and dynamic responses of the functionally graded curved beams. An analytical study to analyse the free vibration responses of laminated shallow curved beams based on the trigonometric shear deformation curved beam theory is performed by Jun *et al*. (2014). In this study, the equations of motion for linear free vibrations of shallow arches are solved using the dynamic stiffness method. Based on the nonlocal strain gradient theory, a linear free vibration analysis for deep and shallow FGM curved nano beams is performed by Hosseini and Rahmani (2016). According to the first-order Timoshenko curved beam model, differential equations of motion are obtained using the Hamilton principle. In this work, the equations of motion of the FG curved nanobeams are solved analytically by employing the Navier solution procedure. Based on the classical shallow arch theory, Keibolahi *et al*. (2018) studied the nonlinear dynamic snap-through response of a homogeneous isotropic shallow arch subjected to thermal shock. In this study, Ritz method is used to solve the nonlinear differential equations of motion. Also, free vibration analysis of FGM deep curved nanobeams has been investigated by Rahmani *et al*. (2018). In this work, governing equations of FGM deep curved nanobeams are obtained based on the modified couple stress and first-order shear deformation beam theories. Tornabene *et al*. (2019) performed an investigation on the free vibration responses of shear deformable laminated composite arches and flat beams with variable thickness using the refined shear deformation theories. Babaei *et al*. (2019c, d) have studied the large amplitude free vibration analysis for FGM shallow panels/arches resting on nonlinear hardening or softening elastic foundation by employing an analytical approach as a two-step perturbation technique. Finally, Fariborz and Batra (2019) investigated the free vibration behavior of bi-directional functionally graded circular arches based on the shear deformation theory by employing a logarithmic function. In this study, the equations of motion are solved for different types of boundary conditions employing the generalized differential quadrature method (GDQM).

The current research develops the literature on the analysis of the FGM curved tubes. The large amplitude free vibration characteristics of functionally material curved tubes are analysed where the properties are graded across the thickness. Properties of the tube are considered to be temperature and position dependent. The governing equations of the tube are established using the higher order tube theory and von Kármán types of kinematic assumptions. For shallow tubes with both ends simply supported and immovable in axial direction, the equations governing the large amplitude free vibrations of the tube in thermal environment are extracted. These equations are solved by means of the two step perturbation technique. The closed form expressions are derived for the small and large amplitude vibrations of curved FGM pipes. Numerical results are given to explore the temperature dependence, thermal environment, power law index, and geometrical characteristics of the FGM curved tube.

2. Basic equations

Consider a shallow curved tube with circular cross-section made of temperature dependent functionally graded material from a mixture of ceramic and metal. For elastic curved tubes, the radius of curvature is R, axial curved length is L, and boundary conditions at both ends are immovable simply supported. Annular cross-section of the tube with inner radius a, and outer radius b is referred to both polar coordinates system and Cartesian coordinates system. Schematic and geometric characteristics of the FGM shallow curved tubes are illustrated in Fig. 1.

Also, the following relationship between the Cartesian and polar coordinates systems for annular cross-section of the FG shallow curved tube are expressed as

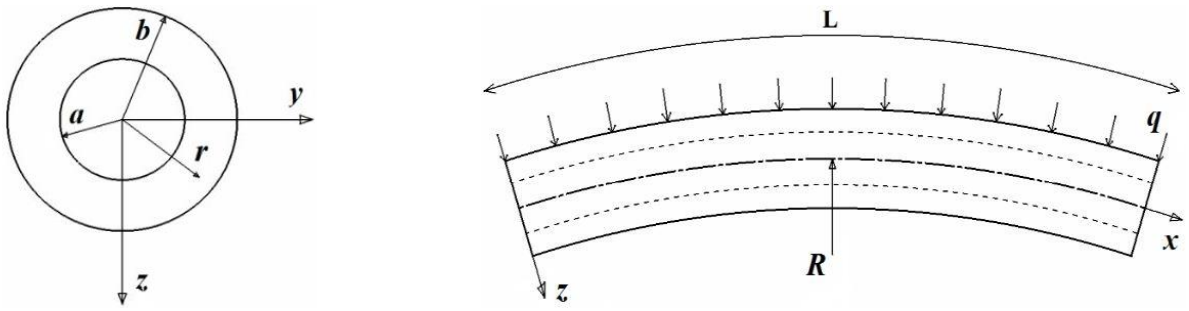

Fig. 1 Schematic and geometric characteristic of the FGM shallow curved tube

$$y = r\cos\theta, \quad z = r\sin\theta, \quad r^2 = y^2 + z^2, \\ a \le r \le b, \quad 0 \le \theta \le 2\pi. \tag{1}$$

Here, y and z are the variables associated with the Cartesian coordinates system, and θ and r, respectively, represent the circumferential and radial directions for the annular cross-section of curved tube.

Mechanical and thermal properties of the functionally graded material curved tube should be defined according to a proper homogenization method. Based on the Voigt rule for FGMs, thermomechanical material properties of the FGM curved tubes are assumed to be the linear function of the volume fractions of ceramic V_c and metal V_m constituents. Thus, as a function of radial coordinate, a non-homogeneous property of the FGM shallow curved tube, $P_f(r,T)$, may be expressed in the following form (Shen 2009, Duc 2013, 2016, 2018, Duc and Cong 2018, Duc *et al*. 2016, 2017, 2018, 2019)

$$P_f(r,T) = P_m(T) + P_{cm}(T)\, V_c(r), \\ P_{cm}(T) = P_c(T) - P_m(T) \tag{2}$$

Here, the subscripts m and c represent the properties of metal and ceramic constituents, respectively. The material properties such as Young's modulus $E(r,T)$, mass density $\rho(r,T)$, thermal expansion coefficient $\alpha(r,T)$ are temperature-dependent. Temperature dependence of the functionally graded properties are assumed to follow the Touloukian model as (Shen 2009, Duc 2016)

$$P(T) = P_0(P_{-1}T^{-1} + 1 + P_1T + P_2T^2 + P_3T^3) \tag{3}$$

where T is the temperature within the shallow curved tube and $P_i(i = 0, \pm 1,2,3)$ are functionally graded material property constants. Obviously, metal rich surface is at the inner surface of the tube $r = a$ and ceramic rich surface is at the outer surface of the tube $r = b$.

A power law distribution of the constituents across the curved tube thickness (radial direction) may be used to represent the ceramic volume fraction V_c and metal volume fraction V_m such as

$$V_c = \left(\frac{r-a}{b-a}\right)^N, \quad V_m = 1 - V_c \tag{4}$$

where N is a positive constant $0 \le N \le \infty$ which is called the volume fraction index of functionally graded materials and dictates the material property dispersion profile.

3. Kinematic equations

In the present study, it is assumed that the FGM curved tube only vibrates in the $x - z$ plane. Displacement field of a shallow curved tube is expressed based on the higher order shear deformation tube theory. The displacement components of the curved tube may be written as (Zhang and Fu 2013)

$$u_1(x,y,z,t) = \left(1 - \frac{z}{R}\right) u(x,t) \\ + z\{\varphi(x,t) + r^{-2}\psi_1(x,t) + r^2\psi_2(x,t)\}, \\ u_2(x,y,z,t) = 0, \\ u_3(x,y,z,t) = w(x,t). \tag{5}$$

In the above equations $u_i(i = 1,2,3)$ are the arbitrary point displacements of a shallow curved tube with $z/R \ll 1$, which are parallel to a set of axes (x,y,z), respectively. Also, $u(x,t)$ and $w(x,t)$, respectively, indicate the displacements at the central axes of the shallow FG curved tube in the $x-$ and $z-$ directions, and $\varphi(x,t)$ is the circular cross-section rotation of tube in the plane of its curvature.

To eliminate two unknown functions $\psi_1(x,t)$ and $\psi_2(x,t)$ in the above displacement field, shear strain component in the $r - x$ plane of shallow curved FGM tube is expressed as (Zhang and Fu 2013)

$$\gamma_{rx} = \frac{z}{r}\left[\varphi(x,t) + \frac{\partial w(x,t)}{\partial x} + \frac{\psi_1(x,t)}{r^2} + 3r^2\psi_2(x,t)\right] \tag{6}$$

Due to the absence of shear stresses and tangential tractions on the inner and outer surfaces of FGM curved tube, the shear strain should be vanished on the surfaces. From this boundary condition for the inner and outer surfaces (at: $r = a, b$), shear strain is vanished $\gamma_{rx} = 0$. Hence, two unknown functions $\psi_1(x,t)$ and $\psi_2(x,t)$ are determined to be

$$\psi_1(x,t) = \frac{a^2b^2}{a^2+b^2}\left[\frac{\partial w(x,t)}{\partial x} + \varphi(x,t)\right], \\ \psi_2(x,t) = \frac{-1}{3(a^2+b^2)}\left[\frac{\partial w(x,t)}{\partial x} + \varphi(x,t)\right]. \tag{7}$$

Finally, by substituting Eq. (7) into Eq. (5), the displacement field for FG curved tube can be written as

$$\begin{aligned} u_1(x,r,\theta,t) &= u(x,t) + F(r,\theta)\frac{\partial w(x,t)}{\partial x} \\ &\quad +[F(r,\theta)+r\sin\theta]\,\varphi(x,t), \\ u_3(x,r,\theta,t) &= w(x,t). \end{aligned} \tag{8}$$

in which

$$F(r,\theta) = \frac{r\sin\theta}{a^2+b^2}\left(\frac{a^2b^2}{r^2} - \frac{r^2}{3}\right). \tag{9}$$

Based on the von Kármán type of geometrical nonlinearity and higher order shear deformation tube theory, the strain-displacement components of shallow curved FGM tubes can be expressed as follow (Babaei *et al*. 2019e)

$$\begin{aligned} \varepsilon_x &= \frac{\partial u}{\partial x} - \frac{w}{R} + \frac{1}{2}\left(\frac{\partial w}{\partial x}\right)^2 + F\frac{\partial^2 w}{\partial x^2} + (F+z)\frac{\partial \varphi}{\partial x}, \\ \gamma_{xy} &= \frac{\partial F}{\partial y}\left(\frac{\partial w}{\partial x} + \varphi\right), \\ \gamma_{xz} &= \left(1 + \frac{\partial F}{\partial z}\right)\left(\frac{\partial w}{\partial x} + \varphi\right). \end{aligned} \tag{10}$$

Here, ε_x represents the normal strain of an arbitrary point of the curved tube in the axial direction. Also, γ_{xy} and γ_{xy} denote the shear strain components.

4. Constitutive equations

Based on the uncoupled thermoelasticity, the constitutive equations for the FGM shallow curved tubes in thermal environment are expressed as (Hetnarski and Eslami 2019)

$$\begin{aligned} \sigma_x &= E(r,T)[\varepsilon_x - \alpha(r,T)\Delta T], \\ \tau_{xy} &= \frac{E(r,T)}{2(1+\nu)}\gamma_{xy}, \\ \tau_{xz} &= \frac{E(r,T)}{2(1+\nu)}\gamma_{xz}, \end{aligned} \tag{11}$$

in which ΔT indicates the temperature difference from reference value of temperature (room temperature) which is set equal $T_0 = 300K$.

Based on the higher order shear deformation tube theory, the axial force and moment resultants are obtained from the stress components by integrating stresses and their moments through the following equations

$$(N_x, M_x, P_x) = \int_a^b \int_0^{2\pi} [\sigma_x, F\sigma_x, (F+z)\sigma_x] r d\theta dr \tag{12}$$

Also, shear force resultant can be expressed as

$$Q_x = \int_a^b \int_0^{2\pi} \left[\frac{\partial F}{\partial y}\tau_{xy} + \left(1 + \frac{\partial F}{\partial z}\right)\tau_{xz}\right] r d\theta dr \tag{13}$$

Substituting Eq. (10) into Eq. (11) with the aid of Eqs. (12) and (13), one obtains the stress resultants in terms of the central axes displacements of shallow curved FGM tube as

$$\begin{Bmatrix} N_x \\ M_x \\ P_x \\ Q_x \end{Bmatrix} = \begin{bmatrix} E_1 & 0 & 0 & 0 \\ 0 & E_2 & E_3 & 0 \\ 0 & E_3 & E_4 & 0 \\ 0 & 0 & 0 & E_5 \end{bmatrix} \begin{Bmatrix} \varepsilon_0 \\ \varepsilon_1 \\ \varepsilon_2 \\ \gamma_0 \end{Bmatrix} - \begin{Bmatrix} N^T \\ M^T \\ P^T \\ 0 \end{Bmatrix} \tag{14}$$

in which

$$\begin{aligned} \varepsilon_0 &= \frac{\partial u}{\partial x} - \frac{w}{R} + \frac{1}{2}\left(\frac{\partial w}{\partial x}\right)^2, \quad \varepsilon_1 = \frac{\partial^2 w}{\partial x^2}, \\ \varepsilon_2 &= \frac{\partial \varphi}{\partial x}, \qquad\qquad\qquad \gamma_0 = \frac{\partial w}{\partial x} + \varphi\,. \end{aligned} \tag{15}$$

In the above equations, the constant coefficients $E_i (i = 1,2,3,4,5)$ are calculated as follow

$$\begin{aligned} &(E_1, E_2, E_3, E_4) \\ &\quad = \int_a^b \int_0^{2\pi} E(r,T)[1, F^2, F(F+z), (F+z)^2] r d\theta dr, \\ &E_5 = \int_a^b \int_0^{2\pi} \frac{E(r,T)}{2(1+\nu)}\left[\left(\frac{\partial F}{\partial y}\right)^2 + \left(1 + \frac{\partial F}{\partial z}\right)^2\right] r d\theta dr. \end{aligned} \tag{16}$$

Besides, N^T, M^T, and P^T are the thermal force and thermal moments resultants which are given by

$$\begin{aligned} &(N^T, M^T, P^T) \\ &= \int_a^b \int_0^{2\pi} E(r,T)\alpha(r,T)(T - T_0)(1, F, F+z) r d\theta dr \end{aligned} \tag{17}$$

5. Equations of motion

The equations of motion for FGM shallow curved tubes based on the higher order shear deformation tube theory may be derived by applying the Hamilton principle

$$\int_{t_1}^{t_2} (\delta K - \delta V - \delta U)\, dt = 0 \tag{18}$$

Using the stress resultants introduced in Eq. (14), total virtual strain energy of the FGM shallow curved tube δU can be written as

$$\begin{aligned} \delta U &= \int_0^L \int_a^b \int_0^{2\pi} \big[\sigma_x\, \delta\varepsilon_x + \tau_{xy}\, \delta\gamma_{xy} \\ &\qquad + \tau_{xz}\, \delta\gamma_{xz}\big] r d\theta dr dx \\ &= \int_0^L (N_x\, \delta\varepsilon_0 + M_x\, \delta\varepsilon_1 + P_x\, \delta\varepsilon_2 + Q_x\, \delta\gamma_0)\, dx \end{aligned} \tag{19}$$

Virtual potential energy of the external applied loads for shallow curved tube under uniform transverse pressure load q_0 can be written as (Babaei *et al*. 2019f)

$$\delta V = -\int_0^L q_0\, \delta w\, dx \tag{20}$$

Using the displacement field introduced in Eq. (8), the virtual kinetic energy δK for FGM shallow curved tube in thermal environment is given by

$$\begin{aligned}\delta K &= \int_0^L \int_a^b \int_0^{2\pi} \rho(r,T)\left[\frac{\partial u_1}{\partial t}\delta\left(\frac{\partial u_1}{\partial t}\right)\right. \\ &\quad \left. + \frac{\partial u_3}{\partial t}\delta\left(\frac{\partial u_3}{\partial t}\right)\right] r d\theta dr dx \\ &= \int_0^L \left[I_0 \frac{\partial w}{\partial t}\delta\left(\frac{\partial w}{\partial t}\right) + \left(I_1 \frac{\partial^2 w}{\partial x\,\partial t} + I_2 \frac{\partial \varphi}{\partial t}\right)\right. \\ &\quad \left. \delta\left(\frac{\partial^2 w}{\partial x\,\partial t}\right) + \left(I_2 \frac{\partial^2 w}{\partial x\,\partial t} + I_3 \frac{\partial \varphi}{\partial t}\right)\delta\left(\frac{\partial \varphi}{\partial t}\right)\right] dx\end{aligned} \tag{21}$$

In the above equation, the axial inertia is ignored and higher order inertia terms $I_i (i = 0,1,2,3)$ are defined by

$$\begin{aligned}&\langle I_0, I_1, I_2, I_3\rangle \\ &= \int_a^b \int_0^{2\pi} \rho(r,T)\langle 1, F^2, F(F+z), (F+z)^2\rangle r d\theta dr\end{aligned} \tag{22}$$

Substituting Eqs. (19)-(21) into Eq. (18) and by means of the suitable mathematical simplifications, the expressions for the equations of motion of the FGM shallow curved tubes are

$$\begin{aligned}&\delta u: \frac{\partial N_x}{\partial x} = 0, \\ &\delta w: \frac{\partial^2 M_x}{\partial x^2} - \frac{\partial}{\partial x}\left(N_x \frac{\partial w}{\partial x}\right) - \frac{\partial Q_x}{\partial x} - \frac{N_x}{R} + I_0 \frac{\partial^2 w}{\partial t^2} \\ &\quad - I_1 \frac{\partial^4 w}{\partial x^2\,\partial t^2} - I_2 \frac{\partial^3 \varphi}{\partial x\,\partial t^2} = q_0, \\ &\delta\varphi: \frac{\partial P_x}{\partial x} - I_2 \frac{\partial^3 w}{\partial x\,\partial t^2} - I_3 \frac{\partial^2 \varphi}{\partial t^2} - Q_x = 0.\end{aligned} \tag{23}$$

To eliminate the central axes displacement, the first of Eqs. (23) is integrated to give

$$N_x = E_1\left(\frac{\partial u}{\partial x} + \frac{1}{2}\left(\frac{\partial w}{\partial x}\right)^2 - \frac{w}{R}\right) - N^T = c_1 \tag{24}$$

Also, integrating Eq. (24) yields

$$u(x,t) = \frac{c_1}{E_1}\, x + \int_0^x \left(\frac{N^T}{E_1} - \frac{1}{2}\left(\frac{\partial w}{\partial x}\right)^2 + \frac{w}{R}\right) dx + c_2 \tag{25}$$

where c_1 and c_2 are two constants of integration. For shallow curved tube with immovable simply supported ends, boundary conditions for axial displacement can be written as $u(0,t) = u(L,t) = 0$. Thus, from immovable end conditions the constant c_1 may be obtained in the following form

$$c_2 = 0, \quad c_1 = \frac{1}{L}\int_0^L \left(\frac{E_1}{2}\left(\frac{\partial w}{\partial x}\right)^2 - E_1 \frac{w}{R} - N^T\right) dx \tag{26}$$

The equations of motion in terms of the displacement components of an FGM shallow curved tube with immovable simply supported ends may be obtained by substituting Eq. (14) into Eq. (23). The resulting equations of motion are

$$\begin{aligned}&N_x = \frac{E_1}{L}\int_0^L \left(\frac{1}{2}\left(\frac{\partial w}{\partial x}\right)^2 - \frac{w}{R}\right) dx - N^T, \\ &\frac{\partial^2}{\partial t^2}\left(I_0 w - I_1 \frac{\partial^2 w}{\partial x^2} - I_2 \frac{\partial \varphi}{\partial x}\right) - N_x\left(\frac{\partial^2 w}{\partial x^2} + \frac{1}{R}\right) \\ &\quad + E_2 \frac{\partial^4 w}{\partial x^4} + E_3 \frac{\partial^3 \varphi}{\partial x^3} - E_5\left(\frac{\partial^2 w}{\partial x^2} + \frac{\partial \varphi}{\partial x}\right) = q_0, \\ &\frac{\partial^2}{\partial t^2}\left[I_2 \frac{\partial w}{\partial x} + I_3 \varphi\right] = E_3 \frac{\partial^3 w}{\partial x^3} + E_4 \frac{\partial^2 \varphi}{\partial x^2} - E_5\left(\frac{\partial w}{\partial x} + \varphi\right)\end{aligned} \tag{27}$$

Here, temperature field of the FGM shallow curved tube is of the uniform temperature rise type and is not a function of x. Thus, derivations of the thermal moments M^T and P^T in the above equations are not displayed.

Also, for the sake of generality, the following non-dimensional quantities are introduced as

$$\begin{aligned}&(A_1, A_2, A_4) = \frac{1}{D}(E_2, E_3, E_4), \\ &(A_3, A_5) = \frac{L^2}{D\pi^2}(E_1, E_5), \\ &W = \frac{w}{L}, \qquad \beta = \frac{L}{R\pi^2}, \qquad \xi = \frac{\pi x}{L}, \\ &\Phi = \frac{\varphi}{\pi}, \qquad \lambda^T = \frac{N^T L^2}{D\pi^2}, \qquad B_0 = \frac{E_0 I_0 L^2}{\rho_0 D\pi^2}, \\ &(B_1, B_2, B_3) = \frac{E_0}{\rho_0 D}(I_1, I_2, I_3), \quad \lambda^q = \frac{q_0 L^3}{D\pi^4}, \\ &\tau = \frac{\pi t}{L}\sqrt{E_0/\rho_0}, \qquad \omega_L = \bar{\omega}_L \frac{L}{\pi}\sqrt{\rho_0/E_0}\end{aligned} \tag{28}$$

in which

$$D = \int_a^b \int_0^{2\pi} E(r,T) z^2 r d\theta dr \tag{29}$$

Here, E_0 and ρ_0, respectively, are the reference values of $E_m(T)$ and $\rho_m(T)$ at room temperature (300K).

Finally, the equations of motion for FGM shallow curved tubes are reduced to two new dimensionless equations as

$$\begin{aligned}&\delta W: A_1 \frac{\partial^4 W}{\partial \xi^4} + A_2 \frac{\partial^3 \Phi}{\partial \xi^3} \\ &\quad + \left\{\lambda^T - \pi A_3 \int_0^\pi \left[\frac{1}{2}\left(\frac{\partial W}{\partial \xi}\right)^2 - \beta W\right] d\xi\right\} \\ &\quad \left(\frac{\partial^2 W}{\partial \xi^2} + \beta\right) - A_5\left[\frac{\partial^2 W}{\partial \xi^2} + \frac{\partial \Phi}{\partial \xi}\right] \\ &\quad + \frac{\partial^2}{\partial \tau^2}\left[B_0 W - B_1 \frac{\partial^2 W}{\partial \xi^2} - B_2 \frac{\partial \Phi}{\partial \xi}\right] = \lambda^q, \\ &\delta\Phi: A_2 \frac{\partial^3 W}{\partial \xi^3} + A_4 \frac{\partial^2 \Phi}{\partial \xi^2} - A_5\left(\frac{\partial W}{\partial \xi} + \Phi\right) \\ &\quad B_2 \frac{\partial^3 W}{\partial \xi\,\partial \tau^2} - B_3 \frac{\partial^2 \Phi}{\partial \tau^2} = 0.\end{aligned} \tag{30}$$

The dimensionless boundary conditions for shallow curved tubes with immovable simply supported ends are

$$at: \xi = 0, \pi: W = M_x = P_x = 0 \tag{31}$$

Also, the dimensionless initial conditions for nonlinear

free vibration analysis of shallow curved tubes are

$$at:\ \tau=0\ :\ W=\frac{\partial W}{\partial \tau}=\Phi=\frac{\partial \Phi}{\partial \tau}=0 \tag{32}$$

6. Solution procedure

An analytical approach is adopted in this section to obtain the closed-form solution for large amplitude free vibration analysis of the FGM shallow curved tubes in thermal environment. According to the two-step perturbation technique (Shen 2013), the closed-form solutions may be obtained by substituting the following series solution into Eq. (30).

$$\begin{aligned} &W(\xi,\tau,\varepsilon)=\sum w_i(\xi,\tau)\varepsilon^i\ ,\quad \lambda^q(\varepsilon)=\sum \lambda_i\varepsilon^i\ ,\\ &\Phi(\xi,\tau,\varepsilon)=\sum \varphi_i(\xi,\tau)\varepsilon^i. \end{aligned} \tag{33}$$

By collecting the terms of small perturbation parameter ε, the following set of differential equations are calculated as

The first-order perturbation equations are

$$\begin{aligned} O(\varepsilon^1):\ & A_1\frac{\partial^4 w_1}{\partial\xi^4}+A_2\frac{\partial^3\varphi_1}{\partial\xi^3}+\lambda^T\frac{\partial^2 w_1}{\partial\xi^2}\\ &-A_5\left(\frac{\partial^2 w_1}{\partial\xi^2}+\frac{\partial\varphi_1}{\partial\xi}\right)+\pi\beta^2A_3\int_0^\pi w_1\,d\xi=\lambda_1,\\ & A_2\frac{\partial^3 w_1}{\partial\xi^3}+A_4\frac{\partial^2\phi_1}{\partial\xi^2}-A_5\left(\frac{\partial w_1}{\partial\xi}+\varphi_1\right)=0. \end{aligned} \tag{34}$$

The second-order perturbation equations are

$$\begin{aligned} O(\varepsilon^2):\ & A_1\frac{\partial^4 w_2}{\partial\xi^4}+A_2\frac{\partial^3\varphi_2}{\partial\xi^3}-A_5\left(\frac{\partial^2 w_2}{\partial\xi^2}+\frac{\partial\varphi_2}{\partial\xi}\right)\\ &-\pi\beta\frac{A_3}{2}\int_0^\pi\left(\frac{\partial w_1}{\partial\xi}\right)^2d\xi+\pi\beta^2A_3\int_0^\pi w_2d\xi\\ &+\lambda^T\frac{\partial^2 w_2}{\partial\xi^2}+\left(\pi\beta A_3\int_0^\pi w_1d\xi\right)\frac{\partial^2 w_1}{\partial\xi^2}=\lambda_2,\\ & A_2\frac{\partial^3 w_2}{\partial\xi^3}+A_4\frac{\partial^2\varphi_2}{\partial\xi^2}-A_5\left(\frac{\partial w_2}{\partial\xi}+\varphi_2\right)=0. \end{aligned} \tag{35}$$

The third-order perturbation equations are

$$\begin{aligned} O(\varepsilon^3):\ & A_1\frac{\partial^4 w_3}{\partial\xi^4}+A_2\frac{\partial^3\varphi_3}{\partial\xi^3}-A_5\left(\frac{\partial^2 w_3}{\partial\xi^2}+\frac{\partial\varphi_3}{\partial\xi}\right)\\ &+\pi\beta^2A_3\int_0^\pi w_3d\xi-\pi\beta A_3\int_0^\pi\frac{\partial w_1}{\partial\xi}\frac{\partial w_2}{\partial\xi}d\xi\\ &+\left\{\pi A_3\int_0^\pi\left[\beta w_2-\frac{1}{2}\left(\frac{\partial w_1}{\partial\xi}\right)^2\right]d\xi\right\}\frac{\partial^2 w_1}{\partial\xi^2}\\ &+\lambda^T\frac{\partial^2 w_3}{\partial\xi^2}+\left(\pi\beta A_3\int_0^\pi w_1d\xi\right)\frac{\partial^2 w_2}{\partial\xi^2}\\ &+\varepsilon^2\left(B_0\frac{\partial^2 w_1}{\partial\tau^2}-B_1\frac{\partial^4 w_1}{\partial\xi^2\,\partial\tau^2}-B_2\frac{\partial^3\varphi_1}{\partial\xi\,\partial\tau^2}\right)\\ &=\lambda_3, \end{aligned} \tag{36}$$

$$\begin{aligned} &A_2\frac{\partial^3 w_3}{\partial\xi^3}+A_4\frac{\partial^2\varphi_3}{\partial\xi^2}-A_5\left(\frac{\partial w_3}{\partial\xi}+\varphi_3\right)\\ &-\varepsilon^2\left(B_2\frac{\partial^3 w_1}{\partial\xi\,\partial\tau^2}+B_3\frac{\partial^2\varphi_1}{\partial\tau^2}\right)=0. \end{aligned} \tag{36}$$

In the next steps, perturbation Eqs. (34) to (36) are solved analytically for large amplitude free vibration responses of the FGM shallow curved pinned tubes.

Simply supported boundary conditions and initial conditions given by Eqs. (31) and (32) may be satisfied when the general solutions of the first-order perturbation Eq. (34) are represented in the following form

$$\begin{aligned} &w_1(\xi,\tau)=A_{10}(\tau)\sin(m\xi)\\ &\varphi_1(\xi,\tau)=B_{10}(\tau)\cos(m\xi),\quad m=1,2,\dots \end{aligned} \tag{37}$$

Substituting Eq. (37) into Eq. (34) yields

$$\begin{aligned} &[(A_1m^4+A_5m^2-m^2\lambda^T)A_{10}+m(A_2m^2+A_5)B_{10}]\\ &\times\sin(m\xi)+\frac{2\pi}{m}A_3\beta^2A_{10}=\lambda_1,\\ &[m(A_2m^2+A_5)A_{10}+(A_4m^2+A_5)B_{10}]\cos(m\xi)=0 \end{aligned} \tag{38}$$

Second of Eq. (38) yields

$$B_{10}(\tau)=-\frac{m(m^2A_2+A_5)}{m^2A_4+A_5}A_{10}(\tau) \tag{39}$$

As a result, by substituting Eq. (39) into the first of Eq. (38), the following solution is obtained

$$\begin{aligned} &\lambda_1\\ &=\left[m^4\left(A_1-A_2\frac{m^2A_2+A_5}{m^2A_4+A_5}+\frac{(A_4-A_2)A_5}{m^2A_4+A_5}\right)-m^2\lambda^T\right]\\ &\times A_{10}(\tau)\sin(m\xi)+\frac{2\pi}{m}A_3\beta^2A_{10}(\tau) \end{aligned} \tag{40}$$

The general solutions of the second-order perturbation Eq. (35) can be written as

$$\begin{aligned} &w_2(\xi,\tau)=A_{20}(\tau)\sin(2m\xi)\,,\\ &\varphi_2(\xi,\tau)=B_{20}(\tau)\cos(2m\xi),\quad m=1,2,\dots \end{aligned} \tag{41}$$

Substituting Eqs. (41) and (37) into Eq. (35) yields

$$\begin{aligned} &\{4(4A_1m^4+m^2A_5-m^2\lambda^T)A_{20}\\ &+2m(4A_2m^2+A_5)B_{20}\}\sin(2m\xi)\\ &=\lambda_2+\frac{\pi^2m^2}{4}A_3\beta(A_{10})^2\\ &+2\pi mA_3\beta(A_{10})^2\sin(m\xi),[2m(4A_2m^2+A_5)A_{20}\\ &+(4A_4m^2+A_5)B_{20}]\cos(2m\xi)=0 \end{aligned} \tag{42}$$

From Eqs. (42), the following solution can be obtained as

$$\begin{aligned} &A_{20}(\tau)=B_{20}(\tau)=0,\\ &\lambda_2=-2\pi mA_3\beta(A_{10})^2\sin(m\xi)-\frac{\pi^2m^2}{4}A_3\beta(A_{10})^2 \end{aligned} \tag{43}$$

Also, the general solutions of the third-order perturbation Eq. (36) can be written as

$$w_3(\xi,\tau) = A_{30}(\tau)\sin(3m\xi),\\ \varphi_3(\xi,\tau) = B_{30}(\tau)\cos(m\xi), \qquad m = 1,2,\ldots \tag{44}$$

Substituting Eqs. (44), (41), and (37) into Eq. (36) yields

$$\begin{aligned}&(81m^4A_1 + 9m^2A_5 - 9m^2\lambda^T)A_{30}\sin(3m\xi)\\ &+\frac{2\pi}{3m}A_3\beta^2A_{30} + \frac{1}{4}\pi^2m^4A_3(A_{10})^3\sin(m\xi))\\ &+\left(B_0 + m^2B_1 - m^2B_2\frac{m^2A_2 + A_5}{m^2A_4 + A_5}\right)\frac{\partial^2A_{10}}{\partial\tau^2}\sin(m\xi)\\ &+(m^3A_2 + mA_5)B_{30}\sin(m\xi) = \lambda_3,\\ &\left[m\left(B_2 - B_3\frac{m^2A_2 + A_5}{m^2A_4 + A_5}\right)\frac{\partial^2A_{10}}{\partial\tau^2} + (m^2A_4 + A_5)B_{30}\right]\\ &\times\cos(m\xi) + (27m^3A_2 + 3mA_5)A_{30}\cos(3m\xi) = 0.\end{aligned} \tag{45}$$

Second of Eq. (45) yields

$$A_{30}(\tau) = 0,\\ B_{30}(\tau) = \frac{-m}{m^2A_4 + A_5}\left(B_2 - B_3\frac{m^2A_2 + A_5}{m^2A_4 + A_5}\right)\frac{\partial^2A_{10}}{\partial\tau^2} \tag{46}$$

Substituting Eq. (46) into the first of Eq. (45) one has

$$\begin{aligned}\lambda_3 = &\left[B_0 + m^2B_1 - m^2B_2\frac{m^2A_2 + A_5}{m^2A_4 + A_5}\right.\\ &\left.+\frac{m^2(m^2A_2 + A_5)}{m^2A_4 + A_5}\left(B_3\frac{m^2A_2 + A_5}{m^2A_4 + A_5} - B_2\right)\right]\\ &\times\frac{\partial^2A_{10}}{\partial\tau^2}\sin(m\xi) + \frac{1}{4}\pi^2m^4A_3(A_{10})^3\sin(m\xi)\end{aligned} \tag{47}$$

From the above closed-form solutions, approximate functions for large amplitude free vibration responses of the FGM shallow curved tubes with immovable pinned ends in thermal environment may be determined as

$$W(\xi,\tau,\varepsilon) = \varepsilon A_{10}(\tau)\sin(m\xi) + O(\varepsilon^4),\\ \Phi(\xi,\tau,\varepsilon) = [\varepsilon B_{10}(\tau) + \varepsilon^3B_{30}(\tau)]\cos(m\xi) + O(\varepsilon^4),\\ \lambda^q(\xi,\tau,\varepsilon) = \lambda_1\varepsilon + \lambda_2\varepsilon^2 + \lambda_3\varepsilon^3 + O(\varepsilon^4) + \cdots \tag{48}$$

By substituting Eqs. (40), (43), and (47) into the third of Eq. (48), the following asymptotic solution may be expressed

$$\begin{aligned}\lambda^q(\xi,\tau,\varepsilon) = &\left[g_0\frac{\partial^2(\varepsilon A_{10})}{\partial\tau^2} + g_1(\varepsilon A_{10}) + g_2(\varepsilon A_{10})^2\right.\\ &\left.+g_3(\varepsilon A_{10})^3\right]\times\sin(m\xi) + g_4(\varepsilon A_{10})\\ &+g_5(\varepsilon A_{10})^2 + O(\varepsilon^4)\end{aligned} \tag{49}$$

in which

$$\begin{aligned}g_0 = &B_0 + m^2B_1 + m^2B_3\left[\frac{m^2A_2 + A_5}{m^2A_4 + A_5}\right]^2\\ &-2m^2B_2\frac{m^2A_2 + A_5}{m^2A_4 + A_5},\\ g_1 = &m^4\left[A_1 - A_2\frac{m^2A_2 + A_5}{m^2A_4 + A_5} + \frac{(A_4 - A_2)A_5}{m^2A_4 + A_5}\right]\\ &-m^2\lambda^T,\end{aligned} \tag{50}$$

$$g_2 = -2\pi mA_3\beta, \qquad g_3 = \frac{1}{4}\pi^2m^4A_3,\\ g_4 = \frac{2\pi}{m}A_3\beta^2, \qquad g_5 = -\frac{1}{4}\pi^2m^2A_3\beta.$$

For nonlinear free vibration problem, applied external uniform pressure is vanished $\lambda^q = 0$. Thus, applying the Galerkin method to Eq. (49) yields

$$\int_0^\pi \lambda^q(\xi,\tau,\varepsilon)\sin(m\xi)\,d\xi = 0 \tag{51}$$

As a result, from Eq. (51), the following Duffing-type equation can be obtained

$$\begin{aligned}&G_0\frac{\partial^2[\varepsilon A_{10}]}{\partial\tau^2} + G_1[\varepsilon A_{10}]\\ &+G_2[\varepsilon A_{10}]^2 + G_3[\varepsilon A_{10}]^3 = 0\end{aligned} \tag{52}$$

in which

$$G_0 = \frac{m\pi}{4}g_0, \qquad G_1 = \frac{m\pi}{4}g_1 + g_4,\\ G_2 = \frac{m\pi}{4}g_2 + g_5, \qquad G_3 = \frac{m\pi}{4}g_3. \tag{53}$$

The analytical closed-form solution of the Duffing-type Eq. (52) is expressed as (Shen 2014a, b)

$$\omega_{NL} = \omega_L\sqrt{1 + \frac{9\ G_1G_3 - 10\ G_2^{\,2}}{12\ G_1^{\,2}}\ W_m^{\,2}} \tag{54}$$

in which $\omega_L = \sqrt{G_1/G_0}$ is the dimensionless linear frequency and ω_{NL} is the dimensionless nonlinear frequency. Also, $W_m = w_m/L$ is the dimensionless amplitude of the FGM shallow curved tube which is obtained from the first of Eqs. (48) as $W_m = \varepsilon A_{10}$. Here, w_m is the mid-span deflection of the curved tube.

7. Results and discussion

Procedure and formulation developed in the previous sections can be used in the rest to analyse the linear and nonlinear free vibration responses of a shallow curved tube made of functionally graded material. Boundary conditions at both ends of FGM shallow curved tube are simply supported and immovable. In the subsequent results, the dimensionless amplitude of FGM shallow curved tube is denoted by w_m/b for the first vibration mode $m = 1$.

Also, a dimensionless parameter is used to obtain the natural frequencies of FGM shallow curved tubes which is $\Omega = \bar{\omega}_L\, b\sqrt{\rho_0/E_0}$. Here, $\bar{\omega}_L$ is the corresponding frequency where from Eq. (28) is obtained as $\bar{\omega}_L = \omega_L(\pi/L)\sqrt{E_0/\rho_0}$. In this section, first the comparison studies are provided. Afterwards, novel numerical results are given to explore the effects of different parameters on the small and large amplitude in-plane free vibration responses of the FGM shallow curved tubes in thermal environment. Except for the comparison study of Table 2, in

the numerical results SUS304 and Si_3N_4 are used as the constituents. The coefficients for these functionally graded constituents are given in Table 1.

7.1 Comparison studies

The comparison studies are developed in this section to assure the validity and accuracy of the developed analytical solutions and numerical results. In these examples, the cases of flat beam/tube made of functionally graded material are considered. The flat beam/tube are a simple case of the shallow curved beams/tubes with $R = \infty$.

In the first example, a solid circular cylindrical beam with $a = 0$ made of functionally graded constituents Al/ZrO_2 is considered. For the sake of comparison, FGM cylindrical beam is not under thermal environment and temperature in the beam is equal to $T = 300K$. Other parameter of the cylindrical beam is $L/b = 10$. Also, material properties for Al are $E = 70$ GPa and $\rho = 2702$ kg/m^3, and for ZrO_2 are $E = 200$ GPa and $\rho = 5700$ kg/m^3. For this example, comparison is performed in Table 2. It is evident that small amplitude frequencies of the FGM flat solid tube are in excellent agreement with those obtained by other investigators.

In the second example, a flat circular tube made of functionally graded Si_3N_4/SUS304 is considered. For the sake of comparison, other parameters of the tube are $a/b = 0.5$, $N = 0$, and $T = 300K$. For this example, comparison is performed for two different L/b ratios in Fig. 2. It is seen that for both geometrical parameters, frequency ratios of the present formulation are in excellent agreement with those of Zhong *et al*. (2016), which accepts the accuracy and correctness of the developed formulation.

7.2 Parametric studies

After validating the developed analytical solution and numerical results, novel numerical results are given for the case of FGM shallow curved tubes with immovable pinned ends in thermal environment.

7.2.1 Influence of temperature change

In this example, the effect of temperature change on the linear and nonlinear free vibration response of the FGM shallow curved tubes is investigated. Results of this study are illustrated in Table 3, and Figs. 3-4. The natural frequencies of the tube are evaluated when the geometrical characteristics of the tube are set equal to $L/R = 0.2$, $L/b = 25$, $a/b = 0.5$. The case of a tube which is linearly graded is considered. Small amplitude frequencies of the

Table 1 Temperature dependent coefficients for SUS304 and Si_3N_4

Material	Property	P_{-1}	P_0	P_1	P_2	P_3
SUS304	$\alpha[1/K]$	0	$12.33e-6$	$8.086e-4$	0	0
	$E[Pa]$	0	$201.04e+9$	$3.079e-4$	$-6.534e-7$	0
	$\rho[kg/m^3]$	0	8166	0	0	0
	ν	0	0.3	0	0	0
Si_3N_4	$\alpha[1/K]$	0	$5.8723e-6$	$9.095e-4$	0	0
	$E[Pa]$	0	$348.43e+9$	$-3.07e-4$	$2.16e-7$	$-8.946e-11$
	$\rho[kg/m^3]$	0	2370	0	0	0
	ν	0	0.3	0	0	0

Table 2 Comparisons of dimensionless natural frequencies for Al/ZrO_2 cylindrical beams with $L/b = 10$

	Source	Ω_1	Ω_2	Ω_3	Ω_4	Ω_5	Ω_6
$N = 0$	Huang and Li (2010b)	0.0890	0.3169	0.6193	0.9557	1.3063	1.6622
	Zhong *et al*. (2016)	0.0889	0.3165	0.6198	0.9590	1.3147	1.6779
	She *et al*. (2018b)	0.0889	0.3163	0.6195	0.9553	1.3079	1.6679
	Present	0.0890	0.3169	0.6205	0.9601	1.3162	1.6797
$N = 1$	Huang and Li (2010b)	0.0902	0.3193	0.6170	0.9459	1.2867	1.6311
	Zhong *et al*. (2016)	0.0900	0.3175	0.6159	0.9462	1.2900	1.6394
	She *et al*. (2018b)	0.0900	0.3172	0.6145	0.9425	1.2836	1.6305
	Present	0.0901	0.3178	0.6166	0.9472	1.2913	1.6410
$N = 5$	Huang and Li (2010b)	0.0885	0.3095	0.5954	0.9075	1.2291	1.5531
	Zhong *et al*. (2016)	0.0883	0.3089	0.5953	0.9097	1.2353	1.5654
	She *et al*. (2018b)	0.0883	0.3087	0.5938	0.9060	1.2293	1.5573
	Present	0.0884	0.3093	0.5959	0.9104	1.2363	1.5665

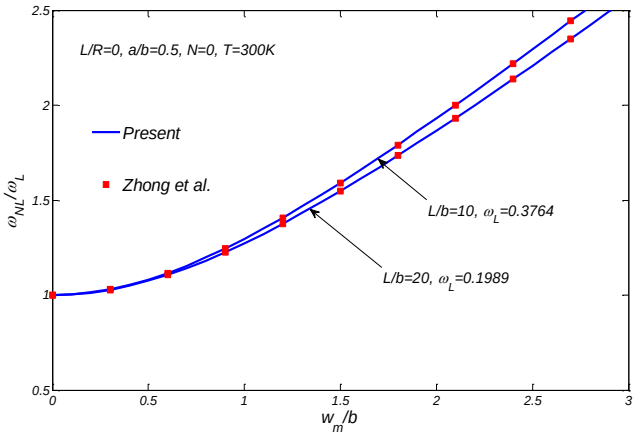

Fig. 2 Comparison between frequency-amplitude curves of this study and Zhong *et al*. (2016) for the flat tubes

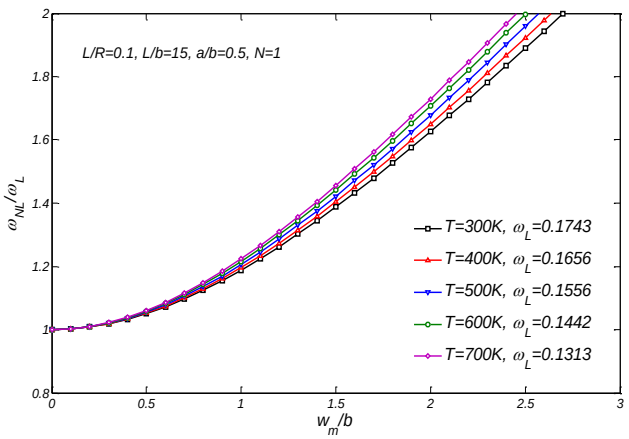

Fig. 3 The effect of temperature change on the frequency-amplitude curves of FGM shallow curved tubes

tube are evaluated and provided in Table 3. It is seen that as the temperature increases, frequencies of the tube decreases. This is expected since with an increase in the temperature, compressive axial force is induced in the tube which results in the stiffness reduction. Also, since properties of the constituents are considered to be temperature dependent, temperature elevation results in the reduction of elasticity modulus which again yields to stiffness reduction.

The effect of thermal environment on the frequency ratios of FGM shallow curved tube is also investigated in this research. The curved tube with characteristics $L/R = 0.1$, $L/b = 15$, $a/b = 0.5$, $N = 1$ are used to generate the results in Fig. 3. It is seen that temperature elevation reduces the frequencies of the shallow curved tube. However, the frequency ratio increases as the temperature elevates.

To better understand the effect of temperature on the small and large amplitude frequencies of a curved tube, the effect of temperature dependence of the constituents is illustrated in Fig. 4. Properties of the tube are $L/R = 0.1$, $L/b = 20$, $a/b = 0.5$, $N = 1$. Two different analysis are shown, which are temperature dependent (TD) and temperature independent (TID). It is seen that under the TD material properties, which is the real state of the properties, natural frequencies decrease which is due to the material degeneration. The ratio of nonlinear to linear frequency ratio also decreases when the assumption of temperature

Table 3 Effect of temperature change on dimensionless natural frequencies of the FGM shallow curved tubes with $L/R = 0.2$, $L/b = 25$, $a/b = 0.5$, $N = 1$

T	Ω_1	Ω_2	Ω_3	Ω_4	Ω_5	Ω_6
300K	0.0168	0.0506	0.1071	0.1781	0.2589	0.3464
400K	0.0154	0.0458	0.1045	0.1747	0.2547	0.3413
500K	0.0138	0.0463	0.1016	0.1710	0.2500	0.3355
600K	0.0119	0.0437	0.0984	0.1668	0.2448	0.3290
700K	0.0095	0.0409	0.0949	0.1623	0.2390	0.3218
800K	0.0061	0.0378	0.0910	0.1573	0.2325	0.3138

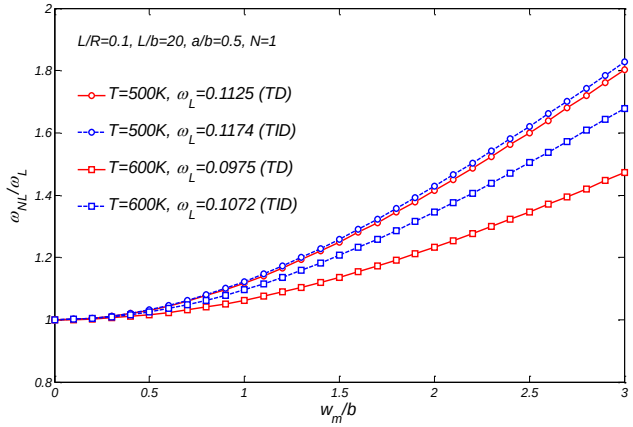

Fig. 4 The effect of temperature dependency on the frequency-amplitude curves for shallow curved tubes

dependent material properties is established.

Since temperature dependence is an important factor in linear and nonlinear free vibrations of FGM shallow curved tubes, in the subsequent results the temperature dependence of the constituents is considered.

7.2.2 Influence of L/R ratio

The next study analyzes the influence of geometrical property L/R on the linear and nonlinear free vibrations of FGM shallow curved tubes. Results of this study are illustrated in Table 4 and Fig. 5.

Table 4 provides the first six frequencies of shallow FGM curved tubes with different L/R ratios. In this example, curved tubes with $L/b = 30$, $a/b = 0.5$, $N = 1$, $T = 300K$ are considered. It is seen that as the L/R ratio increases, the fundamental frequency of the tube increases. Therefore, the frequency of a flat tube is always smaller than a curved tube. However, this effect almost disappears in higher order frequencies of the tube.

The effect of L/R ratio on the frequency ratio is depicted in Fig. 5. The characteristic of the curved tube are as $L/b = 10$, $a/b = 0.5$, $N = 1$, $T = 300K$. Again, it is verified that as the L/R ratio increases, the fundamental

Table 4 Effect of L/R ratio on dimensionless natural frequencies of the FGM shallow curved tubes with $L/b = 30,\ a/b = 0.5,\ N = 1,\ T = 300K$

L/R	Ω_1	Ω_2	Ω_3	Ω_4	Ω_5	Ω_6
0.0	0.0091	0.0354	0.0766	0.1294	0.1910	0.2589
0.1	0.0101	0.0355	0.0766	0.1294	0.1910	0.2589
0.2	0.0127	0.0357	0.0766	0.1294	0.1910	0.2589
0.3	0.0160	0.0360	0.0767	0.1294	0.1910	0.2590
0.4	0.0198	0.0365	0.0768	0.1294	0.1910	0.2590
0.5	0.0238	0.0371	0.0769	0.1295	0.1910	0.2590

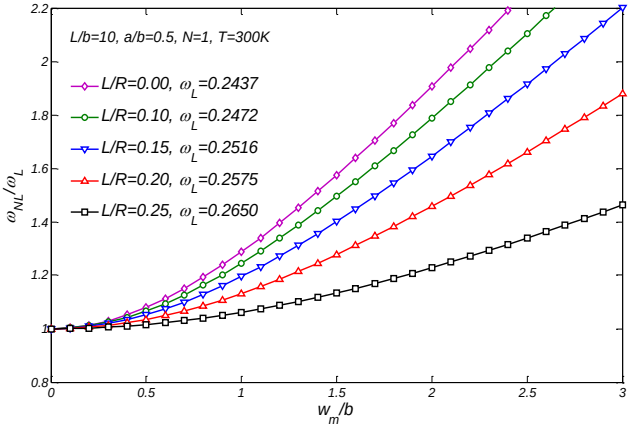

Fig. 5 The effect of L/R ratio on the frequency-amplitude curves of FGM shallow curved tubes in 300K

frequency of the curved tube increases. The frequency ratio of the curved tube decreases when the L/R ratio increases.

7.2.3 Influence of L/b ratio

The effect of geometrical property L/b on linear and nonlinear free vibrations of an FGM shallow curved tube is demonstrated in Table 5 and Fig. 6.

In Table 5, the first six frequencies of the curved tube are tabulated. For the numerical results of this table, tube with parameters $L/R = 0.2,\ a/b = 0.5,\ N = 1,\ T = 300K$ are considered. It is seen that as the L/b ratio increases, the frequencies of the curved tube decreases. This is expected since when the tube becomes longer the effect of boundary conditions almost disappear in the tube thus

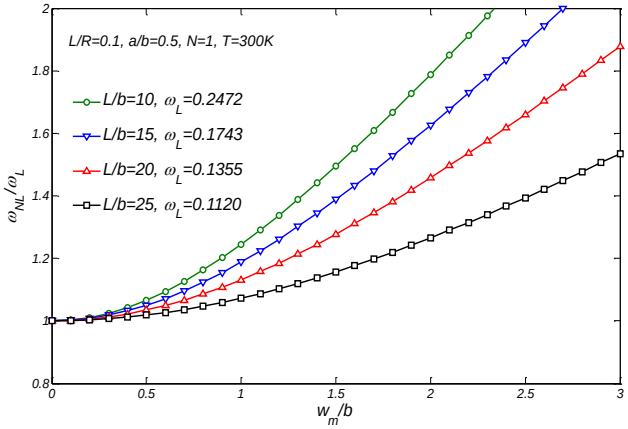

Fig. 6 The effect of L/b ratio on the frequency-amplitude curves of FGM shallow curved tubes in 300K

resulting in loosing the tube stiffness.

The effect of L/b ratio is also depicted on the nonlinear frequency ratio. This study is shown in Fig. 6. For this study, curved tube with parameters $L/R = 0.1,\ a/b = 0.5,\ N = 1,\ T = 300K$ are considered. Again, it is verified that with an increase in the L/b ratio the small amplitude frequency of the tube decreases. However, the nonlinear to linear frequency ratio decreases as this ratio enhances.

7.2.4 Influence of a/b ratio

The next study examines the effect of geometrical property a/b on the linear and nonlinear free vibrations of a shallow FGM curved tube. Results of this study are illustrated in Table 6 and Fig. 7.

The first six linear frequencies of the curved tube are evaluated and provided in Table 6. In this example, curved tubes with parameters $L/R = 0.2,\ L/b = 20,\ N = 1,\ T = 300K$ are examined. It is seen that the influence of a/b ratio on the frequencies is not monotonic. For instance, in the current investigation, the linear fundamental frequency decreases up to $a/b = 0.3$ and then decreases. This conclusion is compatible with the findings of Zhong *et al.* (2016).

Same study is performed to analyse the large amplitude free vibrations of FGM shallow curved tubes. The effect of a/b ratio is analyses in the next investigation where the numerical results are provided in Fig. 7. In this study, curved tubes with $L/R = 0.1,\ L/b = 15,\ N = 1,\ T =$

Table 5 Effect of L/b ratio on dimensionless natural frequencies of the FGM shallow curved tubes with $L/R = 0.2,\ a/b = 0.5,\ N = 1,\ T = 300K$

L/R	Ω_1	Ω_2	Ω_3	Ω_4	Ω_5	Ω_6
15	0.0395	0.1297	0.2590	0.4073	0.5652	0.7283
20	0.0242	0.0768	0.1593	0.2590	0.3691	0.4854
25	0.0168	0.0506	0.1071	0.1781	0.2589	0.3464
30	0.0127	0.0357	0.0766	0.1294	0.1910	0.2589
35	0.0101	0.0265	0.0574	0.0980	0.1462	0.2003
40	0.0084	0.0205	0.0445	0.0766	0.1152	0.1592

Table 6 Effect of a/b ratio on dimensionless natural frequencies of the FGM shallow curved tubes with $L/R = 0.2,\ L/b = 20,\ N = 1,\ T = 300K$

a/b	Ω_1	Ω_2	Ω_3	Ω_4	Ω_5	Ω_6
0.0	0.0248	0.0781	0.1663	0.2775	0.4049	0.5433
0.1	0.0243	0.0765	0.1626	0.2709	0.3946	0.5289
0.3	0.0239	0.0755	0.1589	0.2623	0.3787	0.5038
0.5	0.0242	0.0768	0.1593	0.2590	0.3691	0.4857
0.7	0.0249	0.0798	0.1627	0.2603	0.3657	0.4752
0.9	0.0261	0.0840	0.1685	0.2656	0.3684	0.4736

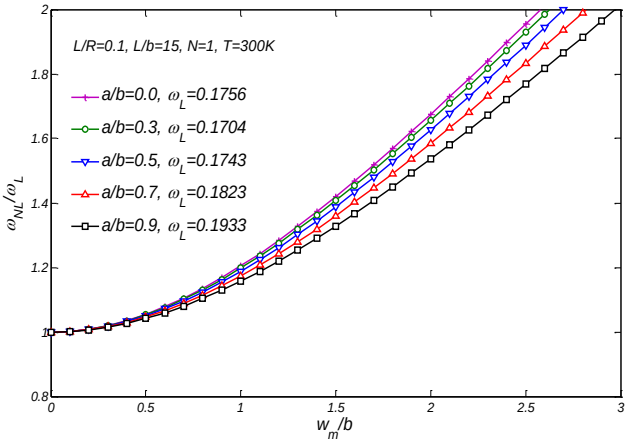

Fig. 7 The effect of a/b ratio on the frequency-amplitude curves of FGM shallow curved tubes in 300 K

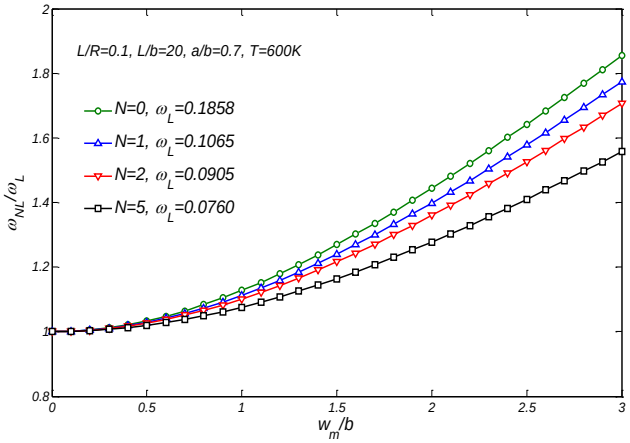

Fig. 8 The effect of power law index N on the frequency-amplitude curves of FGM curved tubes in 600K

$300K$ are analysed. It is observed that as the a/b ratio increases, the nonlinear to linear frequency ratio of the arch decreases.

7.2.5 Influence of the power law index N

Finally, the effect of power law index N on linear and nonlinear free vibrations of a shallow FGM curved tube is demonstrated in Table 7 and Fig. 8.

Table 7 provides the first six frequency parameters of FGM shallow curved tubes where the parameters of the tube are set equal to $L/R = 0.2$, $L/b = 20$, $a/b = 0.5$, $T = 300K$. It is seen that as the power law index N increases the frequency of the curved tube decreases. This is expected since with increasing the power law index the volume fraction of ceramic phase decreases which results in the lower stiffness of the tube since for the constituents of this study elasticity modulus of ceramic material is much higher than the metal material.

Finally, the influence of the power law index of the frequency ratio of FGM shallow curved tubes is depicted in Fig. 8. For this example, curved tubes with $L/R = 0.1$, $L/b = 20$, $a/b = 0.7$, $T = 600K$ are taken into consideration. It is seen that with an increase in the power law index of the curved tube, the frequency ratio decreases permanently. Thus, it may be concluded that the power law index may be used as a controlling parameter in the vibrational characteristics of the FGM curved tubes.

Table 7 Effect of power law index N on dimensionless natural frequencies of the FGM shallow curved tubes with $L/R = 0.2$, $L/b = 20$, $a/b = 0.5$, $T = 300K$

N	Ω_1	Ω_2	Ω_3	Ω_4	Ω_5	Ω_6
0	0.0375	0.1187	0.2464	0.4010	0.5721	0.7533
1	0.0242	0.0768	0.1593	0.2590	0.3691	0.4857
2	0.0213	0.0679	0.1408	0.2289	0.3262	0.4290
3	0.0200	0.0638	0.1323	0.2150	0.3064	0.4031
4	0.0193	0.0614	0.1272	0.2068	0.2948	0.3879
5	0.0188	0.0597	0.1239	0.2014	0.2872	0.3779

8. Conclusions

A large amplitude free vibration response is investigated for the FGM shallow curved tubes in thermal environment. The case of curved tubes with material properties graded across the radial direction are considered. Thermo-mechanical properties of the curved tube are assumed to be temperature dependent. With the aid of a higher order shear deformation tube theory and the von Kármán type of geometrical nonlinearity, the governing dynamic equations for the curved tube are established. These equations of motion are solved for the case of curved tubes which are simply supported in flexure and immovable in axial direction. Closed form solutions are given for the small and large amplitude free vibrations of FGM shallow curved tubes using the two-step perturbation technique. Numerical results are given to discuss the effects of temperature dependence, temperature elevation, power law index and geometrical properties of the curved tube. It is shown that as the temperature elevates, frequencies of the curved tube decrease. Also, the frequency ratio of the curved tube decreases with an increase in the temperature level. Temperature dependence of the constituents results in the lower frequency parameters. For the constituents of this study, as the power law index increases, linear frequencies and also the ratio of frequency of the curved tube decrease.

Acknowledgments

The research received no specific grant from any funding agency in the public, commercial, or not-for-profit sectors.

References

Arefi, M. (2015), "The effect of different functionalities of fgm and FGPM layers on free vibration analysis of the FG circular plates integrated with piezoelectric layers", *Smart Struct. Syst., Int. J.*, **15**(5), 1345-1362. https://doi.org/10.12989/sss.2015.15.5.1345

Babaei, H., Kiani, Y. and Eslami, M.R. (2018a), "Application of two-steps perturbation technique to geometrically nonlinear analysis of long FGM cylindrical panels on elastic foundation under thermal load", *J. Therm. Stress.*, **41**(7), 847-865. https://doi.org/10.1080/01495739.2017.1421054

Babaei, H., Kiani, Y. and Eslami, M.R. (2018b), "Geometrically nonlinear analysis of shear deformable FGM shallow pinned arches on nonlinear elastic foundation under mechanical and thermal loads", *Acta Mech*., **229**(7), 3123-3141. https://doi.org/10.1007/s00707-018-2134-2

Babaei, H., Kiani, Y. and Eslami, M.R. (2018c), "Geometrically nonlinear analysis of functionally graded shallow curved tubes in thermal environment", *Thin-wall. Struct.*, **132**, 48-57. https://doi.org/10.1016/j.tws.2018.08.008

Babaei, H., Kiani, Y. and Eslami, M.R. (2019a), "Thermal buckling and post-buckling analysis of geometrically imperfect FGM clamped tubes on nonlinear elastic foundation", *Appl. Math. Model.*, **71**, 12-30. https://doi.org/10.1016/j.apm.2019.02.009

Babaei, H., Kiani, Y. and Eslami, M.R. (2019b), "Buckling and post-buckling analysis of geometrically imperfect FGM pin-ended tubes surrounded by nonlinear elastic medium under compressive and thermal loads", *Int. J. Struct. Stabil. Dyn.*, **19**(7), 1950089. https://doi.org/10.1142/S0219455419500895

Babaei, H., Kiani, Y. and Eslami, M.R. (2019c), "Large amplitude free vibrations of long FGM cylindrical panels on nonlinear elastic foundation based on physical neutral surface", *Compos. Struct.*, **220**, 888-898. https://doi.org/10.1016/j.compstruct.2019.03.064

Babaei, H., Kiani, Y. and Eslami, M.R. (2019d), "Large amplitude free vibration analysis of shear deformable FGM shallow arches on nonlinear elastic foundation", *Thin-wall. Struct.*, **144**, 106237. https://doi.org/10.1016/j.tws.2019.106237

Babaei, H., Kiani, Y. and Eslami, M.R. (2019e), "Thermally induced large deflection analysis of shear deformable FGM shallow curved tubes using perturbation method", *ZAMM- J. App. Math. Mech.*, **99**(2), Article No. e201800148. https://doi.org/10.1002/zamm.201800148

Babaei, H., Kiani, Y. and Eslami, M.R. (2019f), "Thermomechanical nonlinear In-plane analysis of fix-ended FGM shallow arches on nonlinear elastic foundation using two-step perturbation technique", *Int. J. Mech. Mater. Des.*, **15**(2), 225-244. https://doi.org/10.1007/s10999-018-9420-y

Chen, Y.Z. (2018), "Transfer matrix method for solution of FGMs thick-walled cylinder with arbitrary inhomogeneous elastic response", *Smart Struct. Syst*., *Int. J*., **21**(4), 469-477. https://doi.org/10.12989/sss.2018.21.4.469

Chen, Y., Fu, Y., Zhong, J. and Li, Y. (2017), "Nonlinear dynamic responses of functionally graded tubes subjected to moving load based on a refined beam model", *Nonlinear Dyn.*, **88**(2), 1441-1452. https://doi.org/10.1007/s11071-016-3321-0

Duc, N.D. (2013), "Nonlinear dynamic response of imperfect eccentrically stiffened FGM double curved shallow shells on elastic foundation", *Compos. Struct*., **102**, 306-314. https://doi.org/10.1016/j.compstruct.2012.11.017

Duc, N.D. (2016), "Nonlinear thermal dynamic analysis of eccentrically stiffened S-FGM circular cylindrical shells surrounded on elastic foundations using the Reddy's third-order shear deformation shell theory", *Eur. J. Mech. A-Solid*, **58**, 10-30. https://doi.org/10.1016/j.euromechsol.2016.01.004

Duc, N.D. (2018), "Nonlinear thermo-electro-mechanical dynamic response of shear deformable piezoelectric Sigmoid functionally graded sandwich circular cylindrical shells on elastic foundations", *J. Sandw. Struct. Mater*., **20**(3), 351-378. https://doi.org/10.1177/1099636216653266

Duc, N.D. and Cong, P.H. (2018), "Nonlinear dynamic response and vibration of sandwich composite plates with negative Poisson's ratio in auxetic honeycombs", *J. Sandw. Struct. Mater*., **20**(6), 692-717. https://doi.org/10.1177/1099636216674729

Duc, N.D., Bich, D.H. and Cong, P.H. (2016), "Nonlinear thermal dynamic response of shear deformable FGM plates on elastic foundations", *J. Therm, Stresses*, **39**(3), 278-297. https://doi.org/10.1080/01495739.2015.1125194

Duc, N.D., Nguyen, P.D. and Khoa N.D. (2017), "Nonlinear dynamic analysis and vibration of eccentrically stiffened S-FGM elliptical cylindrical shells surrounded on elastic foundations in thermal environments", *Thin Wall. Struct.*, **117**, 178-189. https://doi.org/10.1016/j.tws.2017.04.013

Duc, N.D., Quang, V.D., Nguyen, P.D. and Chien T.M. (2018), "Nonlinear dynamic response of FGM porous plates on elastic foundation subjected to thermal and mechanical loads using the first order shear deformation theory", *J. Appl. Computat. Mech*., **4**(4), 245-259. https://doi.org/10.22055/jacm.2018.23219.1151

Duc, N.D., Hadavinia, H., Quan, T.Q. and Khoa, N.D. (2019), "Free vibration and nonlinear dynamic response of imperfect nanocomposite FG-CNTRC double curved shallow shells in thermal environment", *Eur. J. Mech. A-Solid*, **75**, 355-366. https://doi.org/10.1016/j.euromechsol.2019.01.024

Eslami, M.R. (2018), *Buckling and Postbuckling of Beams, Plates, and Shells*, Springer, Switzerland.

Fariborz, J. and Batra, R.C. (2019), "Free vibration of bi-directional functionally graded material circular beam using shear deformation theory employing logarithmic function of radius", *Compos. Struct.*, **210**, 217-230. https://doi.org/10.1016/j.compstruct.2018.11.036

Fu, Y., Zhong, J., Shao, X. and Chen, Y. (2015), "Thermal postbuckling analysis of functionally graded tubes based on a refined beam model", *Int. J. Mech. Sci.*, **96-97**, 58-64. https://doi.org/10.1016/j.ijmecsci.2015.03.019

Hetnarski, R.B. and Eslami, M.R. (2019), *Thermal Stresses, Advanced Theory and Applications*, (2th Edition), Springer, Switzerland.

Hosseini, S.A.H. and Rahmani, O. (2016), "Free vibration of shallow and deep curved FG nanobeam via nonlocal Timoshenko curved beam model", *Appl. Phy. A*, **122**, 169-178. https://doi.org/10.1007/s00339-016-9696-4

Huang, Y. and Li, X.F. (2010a), "Buckling of functionally graded circular columns including shear deformation", *Mater. Des.*, **31**(7), 3159-3166. https://doi.org/10.1016/j.matdes.2010.02.032

Huang, Y. and Li, X.F. (2010b), "Bending and vibration of circular cylindrical beams with arbitrary radial nonhomogeneity", *Int. J. Mech. Sci.*, **52**(4), 595-601. https://doi.org/10.1016/j.ijmecsci.2009.12.008

Jun, L., Guangwei, R., Jin, P., Xiaobin, L. and Weiguo, W. (2014), "Free vibration analysis of a laminated shallow curved beam based on Trigonometric shear deformation theory", *Mech. Based Des. Struct.*, **42**(1), 111-129. https://doi.org/10.1080/15397734.2013.846224

Keibolahi, A., Kiani, Y. and Eslami, M.R. (2018), "Dynamic snap-through of shallow arches under thermal shock", *Aerosp. Sci. Tech.*, **77**, 545-554. https://doi.org/10.1016/j.ast.2018.04.003

Malekzadeh, P., Atashi, M.M. and Karami, G. (2009), "In-plane free vibration of functionally graded circular arches with temperature-dependent properties under thermal environment", *J. Sound. Vib.*, **326**(3-5), 837-851. https://doi.org/10.1016/j.jsv.2009.05.016

Malekzadeh, P., Golbahar Haghighi, M.R. and Atashi, M.M. (2010), "Out-of-plane free vibration of functionally graded circular curved beams in thermal environment", *Compos. Struct.*, **92**(2), 541-552. https://doi.org/10.1016/j.compstruct.2009.08.040

Piovan, M.T., Domini, S. and Ramirez, J.M. (2012), "In-plane and out-of-plane dynamics and buckling of functionally graded circular curved beams", *Compos. Struct.*, **94**(11), 3194-3206.

https://doi.org/10.1016/j.compstruct.2012.04.032
Rahmani, O., Hosseini, S.A.H., Ghoytasi, I. and Golmohammadi, H. (2018), "Free vibration of deep curved FG nano-beam based on modified couple stress theory", *Steel Compos. Struct., Int. J.*, **26**(5), 607-620. https://doi.org/10.12989/scs.2018.26.5.607
Shafiei, N. and She, G.L. (2018), "On vibration of functionally graded nanotubes in thermal environment", *Int. J. Eng. Sci.*, **133**, 84-98. https://doi.org/10.1016/j.ijengsci.2018.08.004
She, G.L., Yuan, F.G. and Ren, Y.R. (2017), "Nonlinear analysis of bending, thermal buckling and post-buckling for functionally graded tubes by using a refined beam theory", *Compos. Struct.*, **165**, 74-82. https://doi.org/10.1016/j.compstruct.2017.01.013
She, G.L., Yuan, F.G., Ren, Y.R., Liu, H.B. and Xiao, W.S. (2018a), "Nonlinear bending and vibration analysis of functionally graded porous tubes via a nonlocal strain gradient theory", *Compos. Struct.*, **203**, 614-623. https://doi.org/10.1016/j.compstruct.2018.07.063
She, G.L., Ren, Y.R., Yuan, F.G. and Xiao, W.S. (2018b), "On vibrations of porous nanotubes", *Int. J. Eng. Sci.*, **125**, 23-35. https://doi.org/10.1016/j.ijengsci.2017.12.009
She, G.L., Ren, Y.R., Yuan, F.G. (2019), "Hygro-thermal wave propagation in functionally graded double-layered nanotubes systems", *Steel Compos. Struct., Int. J.*, **31**(6), 641-653. https://doi.org/10.12989/scs.2019.31.6.641
Shen, H.S. (2009), *Functionally Graded Materials Nonlinear Analysis of Plates and Shells*, CRC Press, Boca Raton, FL, USA. https://doi.org/10.1201/9781420092578
Shen, H.S. (2011), "A novel technique for nonlinear analysis of beams on two-parameter elastic foundations", *Int. J. Struct. Stab. Dyn.* **11**(6), 999-1014. https://doi.org/10.1142/S0219455411004440
Shen, H.S. (2013), *A Two-Step Perturbation Method in Nonlinear Analysis of Beams, Plates and Shells*, Wiley & Sons, Singapore.
Shen, H.S. and Wang, Z.X. (2014a), "Nonlinear Analysis of shear deformable FGM beams resting on elastic foundations in thermal environments", *Int. J. Mech. Sci.*, **81**, 195-206. https://doi.org/10.1016/j.ijmecsci.2014.02.020
Shen, H.S. and Wang, H. (2014b), "Nonlinear vibration of shear deformable FGM cylindrical panels resting on elastic foundation in thermal environment", *Compos. Part B*, **60**, 167-177. https://doi.org/10.1016/j.compositesb.2013.12.051
Thai, H.T. and Vo, T.P. (2012), "Bending and free vibration of functionally graded beams using various higher-order shear deformation beam theories", *Int. J. Mech. Sci.*, **62**(1), 57-66. https://doi.org/10.1016/j.ijmecsci.2012.05.014
Tornabene, F., Fantuzzi, N. and Bacciocchi, M. (2019), "Refined shear deformation theories for laminated composite arches and beams with variable thickness: Natural frequency analysis", *Engin. Anal. Boundary Elem.*, **100**, 24-47. https://doi.org/10.1016/j.enganabound.2017.07.029
Wu, C.P. and Li, H.Y. (2012), "Exact solutions of free vibration of rotating multilayered fgm cylinders", *Smart Struct. Syst., Int. J.*, **9**(2), 105-125. https://doi.org/10.12989/sss.2012.9.2.105
Wu, C.P. and Liu, W.L. (2013), "3D buckling analysis of FGM sandwich plates under bi-axial compressive loads", *Smart Struct. Syst., Int. J.*, **13**(1), 111-135. https://doi.org/10.12989/sss.2014.13.1.111
Zhang, D.G. (2014), "Thermal post-buckling and nonlinear vibration analysis of FGM beams based on physical neutral surface and high order shear deformation theory", *Meccanica*, **49**(2), 283-293. https://doi.org/10.1007/s11012-013-9793-9
Zhang, P. and Fu, Y. (2013), "A higher-order beam model for tubes", *Eur. J. Mech. A/Solids*, **38**, 12-19. https://doi.org/10.1016/j.euromechsol.2012.09.009
Zhong, J., Fu, Y., Wan, D. and Li, Y. (2016), "Nonlinear bending and vibration of functionally graded tubes resting on elastic foundations in thermal environment based on a refined beam model", *Appl. Math. Model.*, **40**(17-18), 7601-7614. https://doi.org/10.1016/j.apm.2016.03.031

CC